ISSN 0036-0236, Russian Journal of Inorganic Chemistry, 2016, Vol. 61, No. 3, pp. 296–301. © Pleiades Publishing, Ltd., 2016.
Original Russian Text © O.V. Andreev, Yu.G. Denisenko, E.I. Sal'nikova, N.A. Khritokhin, K.S. Zyryanova, 2016, published in Zhurnal Neorganicheskoi Khimii, 2016, Vol. 61, No. 3, pp. 312–317.

SYNTHESIS AND PROPERTIES OF INORGANIC COMPOUNDS

Specifics of Reactions of Cerium Sulfate and Europium Sulfate with Hydrogen

O. V. Andreev[a], Yu. G. Denisenko[a], E. I. Sal'nikova[a, b], N. A. Khritokhin[a], and K. S. Zyryanova[a]

[a] *Tyumen State University, Tyumen, Russia*
[b] *Agrarian University of South Trans-Urals, Tyumen, Russia*
e-mail: andreev@utmn.ru

Received

Abstract—Reactions of cerium sulfate and europium sulfate with hydrogen have been studied. Diagrams showing the evolution of phase composition of the polycrystalline products of reaction between europium sulfate and hydrogen are constructed. The reaction of $Ce_2(SO_4)_3$ with hydrogen at 600°C consecutively yields Ce_2O_2S and Ce_2O_3 phases. At 800°C the batch is > 95 mol % Ce_2O_3. At 480–500°C, a single-phase sample of $EuSO_4$ is prepared; at 600–1000°C, Eu_2O_2S is prepared; and at 1050°C, the batch is > 95 mol % Eu_2O_2S and up to 5 mol % Eu_2O_3. Atomic-force microscopy shows that europium sulfate grains, which represent agglomerates of particles 10–20 μm in size, are degraded upon reaction with hydrogen into individual oval-shaped particles sized 40–60 × 130–200 nm.

DOI: 10.1134/S0036023616030025

Hydrogen treatment of rare-earth sulfates is a method to produce Ln_2O_2S and $Ln_2O_2SO_4$ compounds [1–6]. Ln_2O_2S compounds are crystal phos-
1 phors [7, 8] and show promise for biolabeling [9, 10]. The literature concerned with the phase composition of products of reaction between rare-earth sulfates and hydrogen is controversial. Earlier publications [3–5] reported that $Ln_2(SO_4)_3$ (Ln = La–Lu or Y) compounds were reduced by hydrogen to oxysulfides Ln_2O_2S in the temperature range of 600–800°C. More recent and more detailed studies of reaction products showed that single-phase Ln_2O_2S samples were formed only for Ln = La, Pr, Nd, or Sm [11]. When $Ln_2(SO_4)_3$ (Ln = Gd–Lu or Y) sulfates are exposed to hydrogen, oxysulfide formation competes with the formation of Ln_2O_3 oxides [12]. Cerium ($4f^25d^06s^2$), samarium ($4f^65d^06s^2$), and europium ($4f^75d^06s^2$), due to the specifics of their electronic structures, have valences III and IV (cerium) and II and III (samarium and europium) and form sulfates of formulas $Ln_2(SO_4)_3$ (Ln = Ce, Sm, or Eu), $LnSO_4$ (Ln = Sm or Eu), and $Ce(SO_4)_2$ [3, 5]. Divalent samarium compounds have not been found to form upon exposure of $Sm_2(SO_4)_3$ to hydrogen. The phase composition of the batch changes in response to increasing temperature by the following scheme: $Sm_2(SO_4)_3 \rightarrow Sm_2O_2SO_4 \rightarrow Sm_2O_2S \rightarrow Sm_2O_3$ [11, 13, 14]. A comparison of the redox potentials and the change of the valence state of ions in aqueous media ($E^\circ_{Sm^{3+}/Sm^{2+}} = -1.15$ V and $E^\circ_{Eu^{3+}/Eu^{2+}} = -0.43$ V) implies that Eu^{3+} is expected to be reduced in flowing hydrogen to Eu^{2+} and to form compounds. We have not found any document concerned with a detailed study of the phase composition of the batch depending on the temperature and time of exposure of $Ce_2(SO_4)_3$ and $Eu_2(SO_4)_3$ to flowing hydrogen.

The diagrams showing the evolution of the phase composition of polycrystalline products of reactions between rare-earth sulfates and hydrogen plotted in the temperature–treatment time space, can serve to determine conditions for the preparation of single-phase $Ln_2O_2SO_4$ or Ln_2O_2S samples or samples of desired phase compositions [12]. Similar diagrams for cerium sulfate and europium sulfate have not been documented.

Our goal was to systematically study the chemistry of heterogeneous reactions between cerium sulfate or europium sulfate and hydrogen.

EXPERIMENTAL

Cerium(III) sulfate was prepared by reacting cerium(IV) oxide (TseO-D type) with sulfuric acid in the presence of hydrogen peroxide. Europium nitrate was prepared by dissolving a calculated weight of europium oxide (EvO-Zh type) in nitric acid (high purity grade 15-3). Europium sulfate(III) was prepared by reacting the europium nitrate solution with concentrated sulfuric acid (chemically pure grade). Thus-

Schemes and equations of chemical reactions of $Ce_2(SO_4)_3$, $Eu_2(SO_4)_3$, and $Eu_2O_2SO_4$ with hydrogen

$Ce_2(SO_4)_3 + H_2$	$Eu_2(SO_4)_3 + H_2$ $Eu_2O_2SO_4 + H_2$
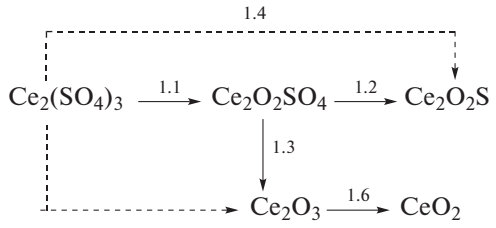	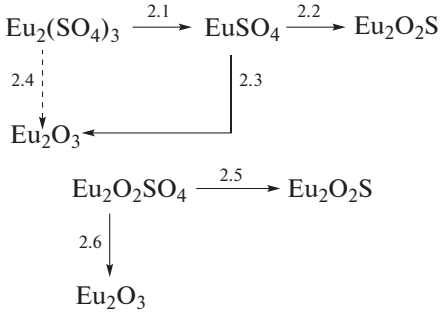
$Ce_2(SO_4)_3 + 6H_2 \rightarrow Ce_2O_2SO_4 + 6H_2O + 2S$ (1.1) $Ce_2O_2SO_4 + 4H_2 \rightarrow Ce_2O_2S + 4H_2O$ (1.2) $Ce_2O_2SO_4 + 3H_2 \rightarrow Ce_2O_3 + 3H_2O + S$ (1.3) $Ce_2(SO_4)_3 + 10H_2 \rightarrow Ce_2O_2S + 10H_2O + 2S$ (1.4) $Ce_2(SO_4)_3 + 9H_2 \rightarrow Ce_2O_3 + 9H_2O + 3S$ (1.5) $2Ce_2O_3 + O_2 \rightarrow 4CeO_2$ (1.6)	$Eu_2(SO_4)_3 + 4H_2 \rightarrow 2EuSO_4 + 4H_2O + S$ (2.1) $2EuSO_4 + 6H_2 \rightarrow Eu_2O_2S + 6H_2O + S$ (2.2) $2EuSO_4 + 5H_2 \rightarrow Eu_2O_3 + 5H_2O + 2S$ (2.3) $Eu_2(SO_4)_3 + 9H_2 \rightarrow Eu_2O_3 + 9H_2O + 3S$ (2.4) $Eu_2O_2SO_4 + 4H_2 \rightarrow Eu_2O_2S + 4H_2O$ (2.5) $Eu_2O_2SO_4 + 3H_2 \rightarrow Eu_2O_3 + 3H_2O + S$ (2.6)

prepared sulfate crystal hydrates were dried in a silica beaker inside a vertical tubular furnace at 700°C for 4–6 h in order to remove water of crystallization and residual acid.

The setup used for hydrogen treatment is described in detail earlier [1]. A sulfate weight of about 10 g (0.1–0.11 mole-equiv.) was pounded and placed in a vertical reactor through which a constant hydrogen flow was passed at a rate of 5.5–6 L/h (0.5–0.6 mole-equiv./h). The treatment temperature was 400–1100°C; the accuracy of temperature maintenance in the reaction zone was ±10°C. At certain synthesis stages, the reactor was taken from the furnace and cooled, and then a sample was taken.

X-ray powder diffraction analysis was carried out on a DRON-7 diffractometer (Ni-filtered CuK_α radiation). X-ray diffraction patterns were indentified with reference to PDF-2. The contents of phases in the batch were determined accurate to ±1 mol %. The water content of sulfates and the total sulfates were determined gravimetrically. Particle sizes and shapes were determined by atomic-force microscopy using an Ntegra Aura scanning probe microscope in a semicontact mode using a V-shaped Si_3N_4 thin-film cantilever. The generator frequency was 153 ± 4 kHz. Scanning was provided by movement of the sample; the maximal useful stage field was ≈13 × 13 μm. Energy-dispersive analysis of particles from various treatment stages was performed on a JEOL JSM 6510 LV scanning electron microscope equipped with an energy-dispersive unit.

RESULTS AND DISCUSSION

Reactions between $Ce_2(SO_4)_3$, $Eu_2(SO_4)_3$, or $Eu_2O_2SO_4$ with hydrogen at temperatures in the range 400–1100°C yield Ce^{III} ($4f^15d^06s^0$) compounds: $Ce_2O_2SO_4$ (table, reaction 1.1), Ce_2O_2S (reactions 1.2 and 1.4), and Ce_2O_3 (reactions 1.3 and 1.5); Eu^{III} ($4f^65d^06s^0$) compounds: Eu_2O_2S (reactions 2.2 and 2.5), Eu_2O_3 (reactions 2.3, 2.4, and 2.6); and Eu^{II} ($4f^75d^05s^0$) compounds: $EuSO_4$ (reaction 2.1).

For reactions 1.1–1.3, 2.1–2.3, 2.5, and 2.6, X-ray powder diffraction detected the direct conversion of the initial polycrystalline compounds into reaction products. The relevant sequence of phase transformations is shown in the diagrams by solid lines. Reactions 1.4, 1.5, and 2.4 in the range of temperatures studied occur in stages. The equations reflect the hypothetic possibility of occurrence of these reactions.

A Ce_2O_3 phase, which is likely formed according to equation 1.3, has high pyrophoricity, and once the reactor is open, it burns in air by reaction 1.6. A CeO_2 phase is detected by X-ray powder diffraction. An analysis of the literature implies that Ce_2O_3 is the only pyrophoric phase of all the feasible reduction products of cerium(III) sulfate [5].

A specific feature of the interaction between $Ce_2(SO_4)_3$ and hydrogen consists in that the products of reactions 1.1–1.3 are formed within close temperature ranges. Starting at 450°C, the products of reactions 1.1 and 1.2 are detected in noticeable amounts in the batch. The treatment of $Ce_2(SO_4)_3$ at 600°C consecutively yields Ce_2O_2S and Ce_2O_3 phases. After 3-h

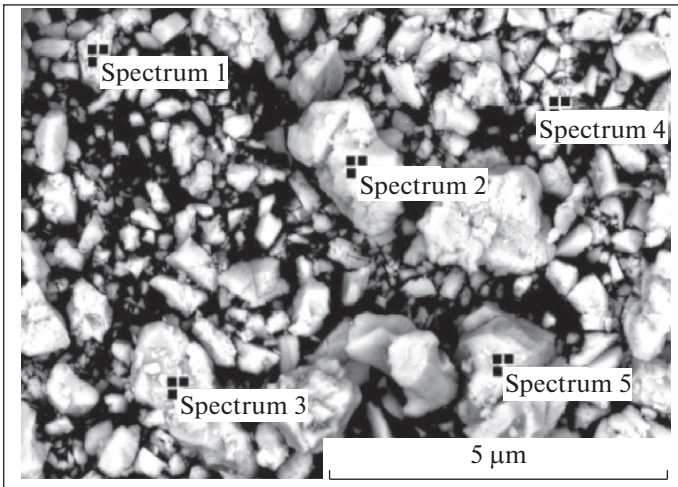

Spectrum	Eu	O	S	Итог
Spectrum 1	61.29	25.78	12.93	100
Spectrum 2	61.25	25.79	12.96	100
Spectrum 3	61.27	25.83	12.90	100
Spectrum 4	61.29	25.79	12.92	100
Spectrum 5	61.30	25.78	12.92	100
Avg.	61.28	25.79	25.79	100
Calcd.	61.27	25.80	25.80	100

Fig. 1. Electron-microscopic image of europium(II) sulfate powder $EuSO_4$, where the sites in which the elemental composition was determined as shown in the table to the right are indicated with (+).

treatment, the batch has the following phase composition: 23 mol % Ce_2O_2S and 77 mol % CeO_2 (Ce_2O_3). The Ce_2O_3 yield increases considerably as the reaction temperature increases. At 800°C after 30-min exposure to flowing hydrogen, the batch has the following composition: 2 mol % Ce_2O_2S and 98 mol % CeO_2 (Ce_2O_3).

The specifics of interaction of $Eu_2(SO_4)_3$ with hydrogen is determined by the concurrency of intermolecular and intramolecular redox reactions and by the absence of $Eu_2O_2SO_4$ in the reaction products. In reaction 2.1, hydrogen reduces the europium cation ($Eu^{3+} \rightarrow Eu^{2+}$) and sulfate ion. In reaction 2.2, sulfate ion is reduced both by hydrogen and by Eu^{2+}. When $Ln_2(SO_4)_3$ (Ln = La, Pr, Nd, Sm, or Gd) is reacted with hydrogen, first the $Ln_2O_2SO_4$ compound is formed by reaction 1.1 [15]. The first reaction product of $Eu_2(SO_4)_3$ with hydrogen is europium sulfate(II) $EuSO_4$, which is detected at 475°C. At a process temperature of 500°C, an impurity-free $EuSO_4$ sample is obtained in 4 h. The strict stoichiometry of this sample was proven by X-ray spectral analysis (Fig. 1) and X-ray powder diffraction (Fig. 2a). In the range 475–600°C, a $Eu_2O_2SO_4$ phase was not detected. At T = 600°C Eu_2O_2S is found in the reaction products. Single-phase Eu_2O_2S samples were prepared in the range 600–1000°C (Fig. 2c). At 1050°C Eu_2O_3 formation was detected (equation 2.3) (Fig. 2d). $Eu_2O_2SO_4$ formation was not observed upon reacting europium sulfate with hydrogen.

The compound $Eu_2O_2SO_4$ was prepared by calcining $Eu_2(SO_4)_3$ under air at 1000°C for 15 h. Reacting europium oxosulfate with hydrogen yields a Eu_2O_2S phase in the range 650–900°C. At T = 950°C, a Eu_2O_3 phase is detected in the products. The scheme of reaction between a $Eu_2O_2SO_4$ phase and hydrogen (table) is consistent with the general phase transformation scheme for $Ln_2O_2SO_4$ (Ln = La, Pr, Nd, or Sm) compounds [11, 15].

Europium(III) sulfate particles represent agglomerates having sizes of 10–20 μm (Fig. 3a), which are formed of initial subgrains sized 1–2 μm, as probed by atomic-force microscopy. A similar structure was earlier observed for $Ln_2(SO_4)_3$ (Ln = La, Nd, or Y) grains [12, 15]. These agglomerates were found to degrade upon the reaction of europium sulfate with flowing hydrogen to individual oval-shaped particles which had homogeneous shape and size distributions (40–60 × 130–190 nm) (Fig. 3b). Such evolution of agglomerates was not observed in the treatment of $Ln_2(SO_4)_3$ (Ln = La, Pr, Nd, or Sm) in flowing hydrogen. Particle coarsen and their grain structure becomes denser in the course of synthesis [15]. In view of a loose grain structure of agglomerates, the reaction of $Eu_2(SO_4)_3$ with hydrogen occurs over the entire bulk of particles. As a result of reaction 2.1, the products of reaction of one-third SO_4^{2-} groups with hydrogen go to the gas phase, and this is likely responsible for the degradation of agglomerates into grains.

Reacting $Eu_2(SO_4)_3$ with hydrogen we obtained samples of five compositions; when the initial substance was $Eu_2O_2SO_4$, samples of three phase compositions were obtained. We plotted the phase compositions of samples versus treatment temperature and treatment time to obtain diagrams showing the evolution of the phase composition of polycrystalline prod-

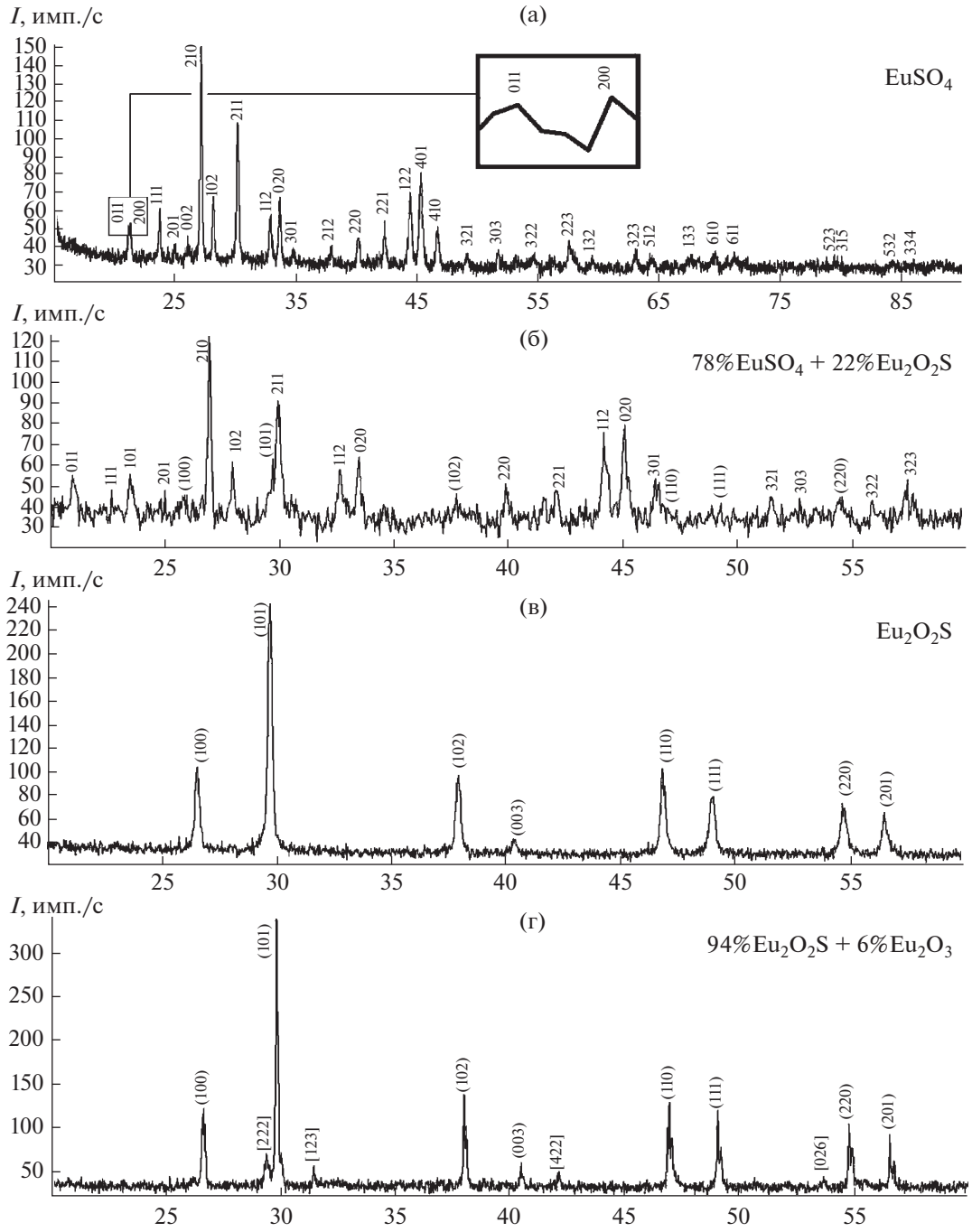

Fig. 2. X-ray diffraction patterns of samples taken from stages of europium sulfate treatment in flowing hydrogen: (a) 240 min at 500°C, (b) 60 min at 600°C, (c) 60 min at 700°C, and (d) 60 min at 1050°C. Miller indices for phases: 011 for $EuSO_4$, (100) for Eu_2O_2S, and [222] for Eu_2O_3.

ucts of reaction between europium sulfates and hydrogen (Fig. 4).

The products of reaction of $Eu_2(SO_4)_3$ and $Eu_2O_2SO_4$ with hydrogen were identified by X-ray powder diffraction at the following process temperatures: 550 and 630°C для Eu_2O_2S, and 1050 and 950°C for Eu_2O_3. The concurrency of intra- and intermolecular interactions involved in the reaction between $Eu_2(SO_4)_3$ and hydrogen favors the steady conversion of all initial and intermediate products to Eu_2O_2S at temperatures of up to 1000°C. $Eu_2O_2SO_4$ reacts with hydrogen by intermolecular interactions, and this is likely responsible for the formation of Eu_2O_3 at as low temperature as 950°C.

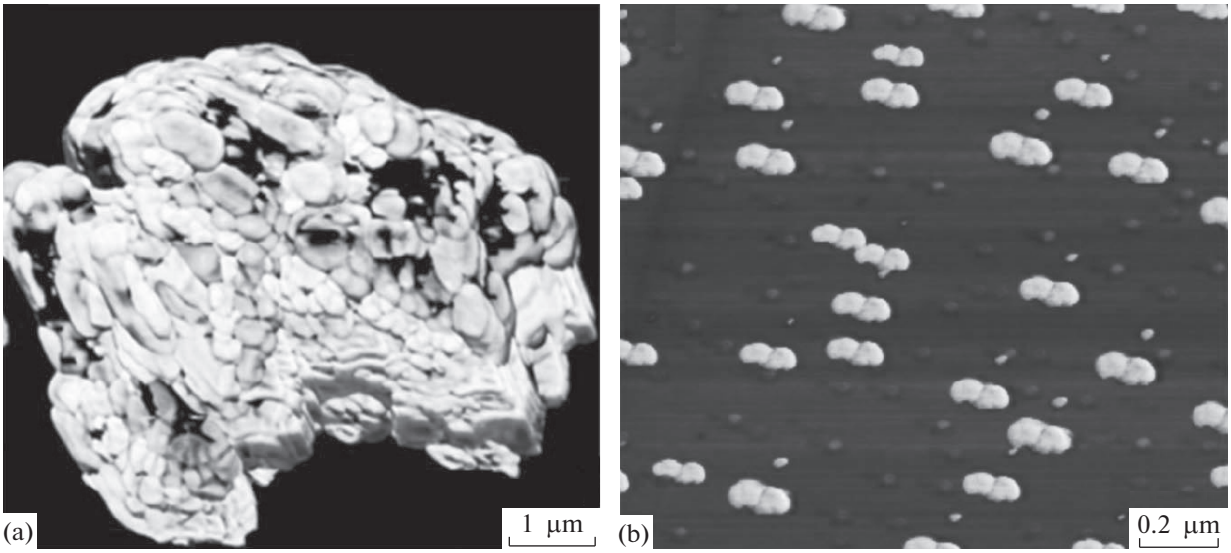

Fig. 3. Images of (a) anhydrous europium sulfate particles: 100 mol % $Eu_2(SO_4)_3$ and (b) europium sulfate(III) treated in flowing hydrogen at 1000°C for 60 min: 100 mol % Eu_2O_2S.

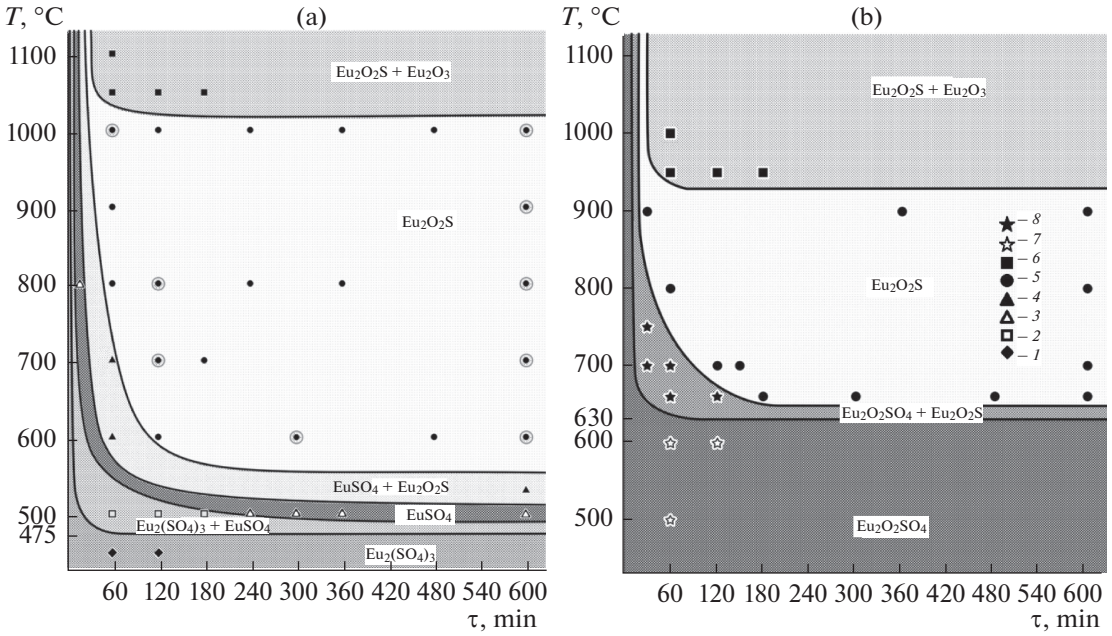

Fig. 4. Diagram showing the evolution of phase composition of polycrystalline products of reactions between (a) $Eu_2(SO_4)_3$ or (b) $Eu_2O_2SO_4$ and hydrogen: (*1*) $Eu_2(SO_4)_3$, (*2*) $Eu_2(SO_4)_3$ + $EuSO_4$, (*3*) $EuSO_4$, (*4*) $EuSO_4$ + Eu_2O_2S, (*5*) Eu_2O_2S, (*6*) Eu_2O_2S + Eu_2O_3, (*7*) $Eu_2O_2SO_4$, and (*8*) $Eu_2O_2SO_4$ + Eu_2O_2S.

The number of phases in the contiguous fields of phase transformation schemes differs by unity, which is responsible for the correspondence of the schemes to the contiguous spaces rule (when two fields of a planar diagram border along a line, they differ from each other by one phase [16]). The positions of phase fields in phase transformation diagrams makes it possible to determine the conditions for preparing single-phase samples of tailored compounds and samples of tailored phase compositions.

ACKNOWLEDGMENTS

This study was supported by the Government Assignment no. 2014/228 (R&D project no. 996).

REFERENCES

1. P. O. Andreev, E. I. Salnikova, and A. A. Kislitsyn, Russ. J. Phys. Chem. **87**, 1482 (2013).
2. E. I. Salnikova, D. I. Kaliev, and P. O. Andreev, Russ. J. Phys. Chem. **85**, 2121 (2011).
3. V. V. Serebrennikov and L. A. Alekseenko, *Lectures on the Chemistry of Rare-Earth Elements* (TGU, Tomsk, 1963) [in Russian].
4. V. A. Batyreva, V. V. Kozik, V. V. Serebrennikov, and G. M. Yakunina, *Syntheses of Rare-Earth Compounds* (TGU, Tomsk, 1983) [in Russian].
5. Yu. D. Tret'yakov, L. I. Martynenko, A. N. Grigor'ev, and A. Yu. Tsivadze, *Inorganic Chemistry. The Chemistry of the Elements: Textbook for High Schools* (Khimiya, Moscow, 2001), Book 1 [in Russian].
6. O. V. Andreev, E. I. Sal'nikova, Yu. G. Denisenko, et al., www.science-education.ru/106-7953.
7. B. V. Mikhitar'yan, Candidate Dissertation in Physics and Mathematics (Stavropol, 2007).
8. Yu. V. Orlovskii, K. K. Pukhov, M. V. Polyachenkova, et al., J. Lumin. **125**, 201 (2007).
9. S. A. Osseni, S. Lechevalier, M. Verest, et al., J. Mater. Chem. **21**, 18365 (2011).
10. M. V. Belobeletskaya, N. I. Steblevskaya, and M. A. Medkov, Vestn. DVO RAN, No. **5**, 33 (2013).
11. E. I. Salnikova, P. O. Andreev, and S. M. Antonov, Russ. J. Phys. Chem. **87**, 1280 (2013).
12. P. O. Andreev, E. I. Salnikova, and I. M. Kovenskiy, Inorg. Mater. **50**, 1018 (2014).
13. O. V. Andreev, A. S. Vysokikh, and V. G. Vaulin, Russ. J. Inorg. Chem. **53**, 1320 (2008).
14. O. V. Andreev, E. I. Sal'nikova, and D. V. Zhuravskii, Vestn. Tyumen. Gos. Univ., No. 3, 215 (2010).
15. E. I. Sal'nikova, Candidate Dissertation in Chemistry (Tyumen State Univ., Tyumen, 2012).
16. L. S. Palatnik and A. I. Landau, *Phase Equilibria in Multicomponent Systems* (Izd–vo Khar'kovsk. Univ., Kharkov, 1961) [in Russian].

Translated by O. Fedorova

SPELL: 1. biolabeling